PHYSICAL REVIEW D VOLUME 45, NUMBER 12 15 JUNE 1992

Resummation in a hot scalar field theory

Rajesh R. Parwani*
Institute for Theoretical Physics, State University of New York at Stony Brook, Stony Brook, New York 11794-3840
(Received 13 January 1992)

A resummed perturbative expansion is used to obtain the self-energy in the high-temperature $g^2\phi^4$ field-theory model up to order g^4. From this the zero-momentum pole of the effective propagator is evaluated to determine the induced thermal mass and damping rate for the bosons in the plasma to order g^3. The calculations are performed in the imaginary-time formalism and a simple diagrammatic analysis is used to identify the relevant diagrams at each order. Results are compared with similar real-time calculations found in the literature.

PACS number(s): 12.38.Mh, 11.10.Jj, 12.38.Cy

I. INTRODUCTION

A well-known [1] problem in high-temperature (T) field theory is the breakdown of the conventional perturbative expansion at some order in the coupling constant (g). This happens because in the regime $T \gg gT \gg m_0$, where m_0 represents any intrinsic zero-temperature masses in the theory, the relevant cutoff for infrared (IR) singularities in loop diagrams is the thermal mass ($\sim gT$) rather than m_0. Higher-loop diagrams then accumulate powers of g in the denominator which can compensate for the usual factors of g in the numerator coming from the Feynman rules. Therefore, to compute consistently to a given order in g, we have to take into account all the relevant higher-loop graphs—these usually form an infinite set.

A practical solution is to resum the perturbation series by systematically including [2,3] all lower-order radiative corrections that are significant (such as the thermal mass) in higher-order calculations. For gauge theories the required resummation of the perturbative expansion into an effective expansion was developed recently by Braaten and Pisarski [3] to compute the gluon damping rate to leading ($\sim g^2T$) order. Subsequently, the effective expansion has been used to compute many other quantities [4]. In all these applications, only one-loop diagrams in the *effective* theory were considered.

To go beyond leading order, one must compute two-loop (and higher) diagrams in the effective expansion. Since this is a tedious exercise in the gauge theories, I will in this paper deal with a toy model, the $g^2\phi^4$ theory, in order to explore some of the technical aspects of higher-loop calculations within the resummation program. As will be discussed in Sec. II, for this model only the self-energy has to be resummed, while the vertex can still be treated perturbatively as in the bare theory [3]. A two-loop calculation in the same model with partial resummation has been considered by Altherr [5]. More recently, a modified perturbation expansion for the model was proposed by Banerjee and Mallik [6] to enable the systematic calculation of the effective mass to higher orders. In [6] a mass parameter was introduced in the beginning and later determined by consistency conditions.

The main difference between [5,6] and this paper is that here the imaginary-time formulation (ITF) will be used to perform the calculations, whereas the real-time formulation (RTF) was employed in [5] and [6]. In the ITF the diagrammatics is the same as at $T=0$ and the power counting of IR divergences is extremely simple. These conveniences of the ITF will be exploited to give a careful account of all the diagrams that can contribute to a given order in g toward the self-energy. Also, instead of introducing a mass parameter as in [6], the resummation will be done in stages so as to make it easier to identify the relevant diagrams and ranges of momenta which can contribute to a particular order in the coupling constant. As an example of an explicit calculation, I will determine the thermal mass and damping rate, for bosons at zero momentum, up to order g^3. The results will be compared with those obtained in the RTF. Of course, as the scalar model is quite popular, some of the formulas and results obtained in this paper, especially in Sec. II, may be found in other publications [3,5–8].

The plan for the rest of the paper is as follows. In Sec. II I will set up the notation and perform the first stage in the resummation of self-energy diagrams. This includes only one-loop one-particle-irreducible (1PI) diagrams. At this stage the self-energy is momentum independent, and so the induced thermal mass is easily obtained to order g^2. Although individual higher-loop 1PI self-energy diagrams in the effective expansion seem to contribute to this order, it is demonstrated that their *sum* does not. Thus perturbative computability is maintained in the effective expansion. The one-loop four-point function is also considered in order to explain why the vertex corrections can be treated perturbatively. In Sec. III the effective Lagrangian of the previous section is used to perform the next stage of the resummation, which includes both one- and two-loop diagrams. The thermal mass is obtained up to order g^3. Again, the sum of

*Address after September 1, 1992: Service de Physique Theorique de Saclay, 91191 Gif-sur-Yvette Cedex, France.

higher-loop diagrams is shown to cancel at this order. The imaginary part of the self-energy is also computed to determine the damping rate to lowest order. The conclusion and a summary is in Sec. IV, while the Appendix contains some technical details.

II. ONE-LOOP DIAGRAMS

The starting point is the following Lagrangian for a hot scalar field (i.e., the intrinsic mass has been set to zero):

$$\mathcal{L}_0=\frac{1}{2}(\partial_\mu\phi)^2+\frac{g^2\mu^{2\epsilon}}{4!}\phi^4 . \tag{2.1}$$

The Lagrangian has been written in D-dimensional Euclidean space, where $D=4-2\epsilon$ and μ is the mass parameter of dimensional regularization. The renormalization counterterms, which have not been displayed, will be determined in the minimal-subtraction scheme [9]. In the imaginary-time formulation of finite-temperature field theory [10,11], the information about the temperature (T) is contained in the energies which are now discrete; for bosons, $p^0=2\pi jT$, where j is an integer. The only change from the zero-temperature Feynman rules is then in the replacement (much of the notation is similar to [12])

$$\int d^Dk/(2\pi)^D\rightarrow \mathrm{Tr}_k\equiv T\sum_{j=-\infty}^{+\infty}\int d^{D-1}k/(2\pi)^{D-1} . \tag{2.2}$$

The sum over the discrete frequencies inside loops is most efficiently performed using the "Saclay" method [12]. Real-time amplitudes are then obtained by analytically continuing [10] the external energies, $p^0\rightarrow -i\omega$. Let $\Delta(K)$ represent a bosonic propagator with mass M and momentum $K^2=(k^0)^2+k^2$:

$$\Delta(K)=\frac{1}{K^2+M^2} . \tag{2.3}$$

For the Lagrangian $\mathcal{L}_0$, the massless propagator will be denoted as $\Delta_0(K)=1/K^2$. In the Scalay method, the propagators inside loops are replaced by their spectral representations

$$\begin{aligned}\Delta(K)&=\int_0^{1/T}d\tau\, e^{ik^0\tau}\Delta(\tau,k) ,\\ \Delta(\tau,k)&=(1/2E_k)[(1+n_k)e^{-E_k\tau}+n_k e^{E_k\tau}] .\end{aligned} \tag{2.4}$$

Here $E_k^2=k^2+M^2$ and $n_k=1/[\exp(E_k/T)-1]$ is the Bose-Einstein distribution function. The expression (2.4) for the noncovariant propagator is valid for $0\le\tau\le 1/T$ and is defined to be periodic in τ with period $1/T$ outside that range. By using the spectral representation of the propagators, it is trivial to do the frequency sums followed by the τ integrals, leaving only the integrations over spatial momenta to be performed [12].

The main calculations in this paper will focus on obtaining consistently the pole of the effective propagator, $1/[P^2-\Pi(p^0,\mathbf{p})]$, where $P^\mu=(p^0,\mathbf{p})$ is the external four-momentum and Π is the 1PI self-energy. For the theory described by (2.1), the diagram in Fig. 1(a) can now be evaluated as described above to determine the self-energy to lowest order:

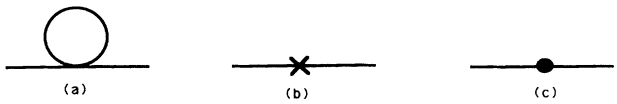

FIG. 1. (a) One-loop self-energy diagram (also called the "bubble"), (b) ultraviolet mass counterterm, and (c) finite two-point interaction ("blob") counterterm induced by the resummation.

$$\begin{aligned}\Pi_0(p^\mu)&=-\frac{g^2\mu^{2\epsilon}}{2}\mathrm{Tr}_k\Delta_0(K)\\ &=-\frac{g^2\mu^{2\epsilon}}{2}\left[\int\frac{d^{D-1}k}{(2\pi)^{D-1}}\frac{1}{2k}+2\int\frac{d^{D-1}k}{(2\pi)^{D-1}}\frac{n_k}{2k}\right].\end{aligned} \tag{2.5}$$

The first integral in (2.5) is the self-energy at $T=0$. It vanishes in dimensional regularization [9], and so there are no ultraviolet (UV) divergences to this order. The second integral in (2.5) represents the matter contribution and is UV finite because of the Bose-Einstein (BE) factor. Putting $\epsilon=0$ then gives the result

$$\Pi_0(p^\mu)=-\frac{g^2T^2}{24} . \tag{2.6}$$

In this paper the induced thermal mass m is defined as the real part of the pole of the Minkowski propagator at zero momentum ($\mathbf{p}=0$). Since the self-energy to this order is independent of momentum, one gets

$$m^2\equiv-\Pi_0=\frac{g^2T^2}{24} . \tag{2.7}$$

To systematically include the effects of this thermal mass, the term $\frac{1}{2}m^2\phi^2$ is added and subtracted [2,3] from (2.1) to define a new effective Lagrangian

$$\mathcal{L}_2=(\mathcal{L}_0+\tfrac{1}{2}m^2\phi^2)-\tfrac{1}{2}m^2\phi^2 . \tag{2.8}$$

The subscript 2 on $\mathcal{L}_2$ is used to remind us that the new Lagrangian now describes a theory with a tree-level mass m with $(m/T)^2\sim g^2$. In (2.8) the quantity in parentheses defines a Lagrangian with free propagator $\Delta_2(K)=1/(K^2+m^2)$. The subtracted term is treated as a new two-point interaction [Fig. 1(c)] of order g^2. The shifting of terms in $\mathcal{L}_0$ to form $\mathcal{L}_2$ corresponds to a resummation of the perturbative expansion.

The next step [3] is to use the effective Lagrangian (2.8) to recalculate the self-energy. In addition to Fig. 1(a), a contribution from the new vertex [Fig. 1(c)] must also be included:

$$\begin{aligned}\Pi_3(p^\mu)&=m^2-\frac{g^2\mu^{2\epsilon}}{2}\mathrm{Tr}_k\Delta_2(K)\\ &=m^2-\frac{g^2}{2}\frac{m^2}{(4\pi)^2}\left[\frac{4\pi\mu^2}{m^2}\right]^\epsilon\Gamma(-1+\epsilon)\\ &\quad-\frac{g^2\mu^{2\epsilon}}{2}\int\frac{d^{D-1}k}{(2\pi)^{D-1}}\frac{2n_k}{2E_k} ,\end{aligned} \tag{2.9}$$

where now $E_k^2=k^2+m^2$. The second term in (2.9) is divergent as $\epsilon\to 0$. This UV divergence is similar to that in $T=0$ field theory. The only difference is that, as a consequence of the resummation, the thermal mass has been introduced into the perturbative calculations. This makes the above divergence temperature dependent [6], albeit in a trivial way—the structure of the divergence is the same as at $T=0$, with the intrinsic mass m_0 replaced by the thermal mass m. Therefore the structure of the mass counterterm will still be the same as for $T=0$, ensuring that the theory is renormalizable even though the counterterms are temperature dependent [see, however, the discussion following (2.17)]. Expanding the divergent term near $\epsilon=0$ gives

$$\frac{g^2}{2}\frac{m^2}{(4\pi)^2}\frac{1}{\epsilon}+\text{finite terms } O\left[g^2m^2\ln\frac{\mu^2}{m^2}\right], \tag{2.10}$$

where, since $m^2\sim(gT)^2$, the finite term is $O(g^4\ln g)$. The mass counterterm vertex [Fig. 1(b)] is thereby fixed to be $-g^2m^2/32\pi^2\epsilon$ at lowest order. The one-loop renormalized self-energy in the theory defined by $\mathcal{L}_2$ is then [see (A4)]

$$\Pi_3^{\text{ren}}=m^2-\frac{g^2}{4\pi^2}\int_0^\infty dk\frac{k^2n_k}{E_k}$$
$$=3m^3/\pi T+O(g^4\ln g)\ . \tag{2.11}$$

The corrected thermal mass M_3 is given by

$$M_3^2=m^2-\Pi_3^{\text{ren}}=m^2(1-3m/\pi T)+O(g^4\ln g)\ . \tag{2.12}$$

Calculating Fig. 1(a) using the propagator $\Delta_2(K)$ is equivalent to summing the infinite set of "daisy" [13] diagrams of Fig. 2 evaluated with the massless propagator $\Delta_0(K)$. This interpretation follows once $\Delta_2(K)=1/(K^2+m^2)$ is expanded in a Taylor series in m^2 about $m^2=0$. Each of the diagrams of Fig. 2 (for $N\geq 1$) is infrared divergent in the theory $\mathcal{L}_0$, but their sum is, as we have seen, infrared finite. Thus summing an infinite set of IR-divergent diagrams has given an IR-finite correction of order g^3 to the mass. The nonanalytic (in g^2) behavior of this correction is a sign of its nonperturbative nature (infinite resummation) when viewed in terms of the original Lagrangian (2.1) [5,11].

Are there any other diagrams in the effective theory (2.8) which can contribute terms of order g^3 to the self-energy? The answer, at first sight, is yes. Even in the *effective* theory, there are *infinitely* many diagrams, other than those in Fig. 1, which can contribute at order g^3, but fortunately for the consistency of the resummation, their *sum* is of order g^4 or higher. Let me term such diagrams "irrelevant" since eventually their finite contributions to the present order in g cancels, although they might be relevant for the UV renormalization of the theory.

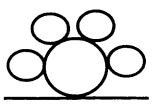

FIG. 2. "Daisy" diagram with $N\geq 1$ attachment of bubbles.

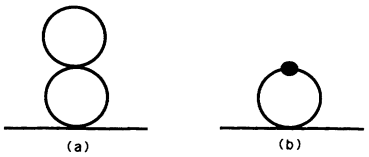

FIG. 3. Set of $N=1$ daisylike diagrams: (a) $N=1$ daisy and (b) insertion of the finite two-point interaction (blob) into the one-loop self-energy (bubble) diagram.

Examples of irrelevant diagrams at order g^3 are given in Fig. 3. Each of the diagrams there is $O(g^2)^2(1/g)\sim g^3$. The factor $(g^2)^2$ comes from the vertices, while $1/g$ comes from the bottom loops as their IR singularity is cut off by the thermal mass. The simplest way to deduce the factor of $1/g$ is to note that the IR behavior of bosonic propagators in loops is dominated by the $j=0$ term in the frequency sum (2.2). That is, to get the leading IR behavior of a diagram, set all the internal energies to zero and then take the $m\to 0$ limit. Consider, for example, Fig. 3(a). Its IR behavior is

$$g^4\text{Tr}_k\text{Tr}_q\{\Delta_2(K)[\Delta_2(Q)]^2\}$$
$$\sim g^4\int\frac{d^3k}{k^2+m^2}\int\frac{d^3q}{(q^2+m^2)^2}$$
$$\to O(g^4)(1)(1/g)=O(g^3)\ . \tag{2.13}$$

However, the sum of the graphs in Fig. 3, with the proper combinatorial factors, is [using Eq. (2.11)]

$$\frac{g^2\mu^{2\epsilon}}{2}\text{Tr}_q[\Delta_2(Q)]^2\left[\frac{g^2\mu^{2\epsilon}}{2}\text{Tr}_k\Delta_2(K)-m^2\right]$$
$$=-\frac{g^2\mu^{2\epsilon}}{2}(\Pi_3)\text{Tr}_q[\Delta_2(Q)]^2$$
$$\sim O(g^2)(g^3)(1/g)=O(g^4)\ . \tag{2.14}$$

The UV-divergent parts, of course, cancel only when all the relevant two-loop and counterterm diagrams are summed (Sec. III). Similarly, although each of the daisylike diagrams shown in Fig. 4 is $O(g^2)^3(1/g^3)\sim g^3$, their sum is easily shown to be

$$-\frac{g^2\mu^{2\epsilon}}{2}\text{Tr}_q[\Delta_2(Q)]^3\left[\frac{g^2\mu^{2\epsilon}}{2}\text{Tr}_k\Delta_2(K)-m^2\right]^2$$
$$\sim\vartheta(g^2)(1/g^3)(g^3)^2=O(g^5)\ . \tag{2.15}$$

In general, each of the daisylike diagrams in Fig. 5 with a fixed number $N\geq 2$ of "bubbles" [Fig. 1(a)] + "blobs" [Fig. 1(c)] is $O(g^3)$, but their sum is

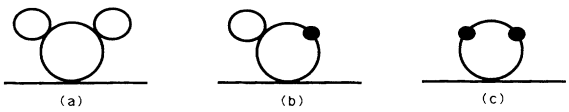

FIG. 4. Set of $N=2$ daisylike diagrams.

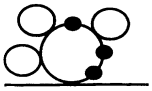

FIG. 5. General daisylike diagram with $N \geq 1$ bubbles + blobs attached.

$$-g^2\mu^{2\epsilon}\mathrm{Tr}_q[\Delta_2(Q)]^{N+1}\sum_{p=0}^{N}\frac{[-g^2\mu^{2\epsilon}\mathrm{Tr}_k\Delta_2(K)]^p}{2^p p!}\frac{(m^2)^{N-p}}{(N-p)!}=-\frac{g^2\mu^{2\epsilon}}{N!}\mathrm{Tr}_q[\Delta_2(Q)]^{N+1}\left[m^2-\frac{g^2\mu^{2\epsilon}}{2}\mathrm{Tr}_k\Delta_2(K)\right]^N$$
$$\sim O(g^2)(1/g^{2N-1})(g^{3N})=O(g^{N+3})\ . \tag{2.16}$$

Thus the set of all daisylike diagrams with $N \geq 2$ is completely irrelevant for the calculations in this paper, which will be performed up to order g^4. It is clear from the above analysis that the presence of the two-point interaction [Fig. 1(c)] is essential. Recall that it was introduced (2.8) to keep us in the same fundamental theory while performing the resummation. We see now how, in the cancellation of contributions from the infinite set of daisy diagrams, it prevents an overcounting of diagrams.

The $N=1$ daisies of Fig. 3 which seem to be relevant at order g^4 will be discussed further in the next section. It is left as an exercise for the interested reader to verify, using the simple power-counting rules for IR singularities illustrated above, that any other 1PI self-energy diagram is individually of order g^4 or higher.

To summarize, the thermal mass including all subleading corrections of order g^3 is completely given by (2.12).

So far, all the results have been written in terms of the renormalized coupling g. The "physical" coupling is determined by evaluating the diagrams of Fig. 6 on shell, which corresponds to soft ($\sim gT$) external momenta. Using the by now familiar power counting, it is seen that each of the diagrams is $O(g^3)$ and hence the radiative correction to the basic four-point vertex is down by a factor of g [7]. Therefore vertex corrections can be treated perturbatively instead of resumming the corrections to form effective four-point vertices. Contrast this with the thermal mass m, which is of the same order as the bare inverse propagator $\Delta_0^{-1}(K)$ for soft momenta and therefore has to be resummed. In the language of [3], for the scalar theory, the only "hard thermal loops" are in the self-energy. In this paper all the results will be left in terms of the renormalized coupling g.

To obtain the complete effective Lagrangian to order g^3, the vertex renormalization counterterm is needed. This is determined as usual by calculating Fig. 6(a) (plus the usual crossed diagrams) at $T=0$. Including first all the counterterms in (2.8) gives

$$\mathcal{L}_2\to\mathcal{L}_2'=(\mathcal{L}_0+m^2\phi^2/2)+\frac{\phi^2}{2!}\left[\frac{g^2m^2}{(4\pi)^2}\frac{1}{2\epsilon}\right]+\frac{g^2\mu^{2\epsilon}}{4!}\phi^4\left[\frac{3g^2}{(4\pi)^2}\frac{1}{2\epsilon}\right]-\left[m^2\phi^2/2+\frac{\phi^2}{2!}\frac{g^2m^2}{(4\pi)^2}\frac{1}{2\epsilon}\right]\ . \tag{2.17}$$

Included in $\mathcal{L}_2'$ is the counterterm [Fig. 7(a)] for loop corrections to the two-point interaction. Note that the net Lagrangian does not contain temperature-dependent counterterms, although pieces of it do because of the resummation [16].

Then, as before, the effects of the thermal mass to order g^3 are included by shifting the mass term in (2.17):

$$\mathcal{L}_3=(\mathcal{L}_0+M_3^2\phi^2/2)+\frac{\phi_2}{2!}\left[\frac{g^2M_3^2}{(4\pi)^2}\frac{1}{2\epsilon}\right]+\frac{g^2\mu^{2\epsilon}}{4!}\phi^4\left[\frac{3g^2}{(4\pi)^2}\frac{1}{2\epsilon}\right]-\left[M_3^2\phi^2/2+\frac{\phi^2}{2!}\frac{g^2M_3^2}{(4\pi)^2}\frac{1}{2\epsilon}\right]\ . \tag{2.18}$$

Note that, for consistency, the mass in the UV counterterms has also been shifted to M_3 in order to cancel the divergences in loop calculations. The Lagrangian (2.18) will be used in the next section to obtain the self-energy up to order g^4. Strictly speaking, the further resummation to obtain $\mathcal{L}_3$ is unnecessary as the $O(g^3)$ correction to m^2 is a perturbative correction, just like the $O(g^3)$

FIG. 6. (a) One-loop correction to the four-point vertex (the diagrams in the crossed channels are not shown) and (b) UV vertex counterterm.

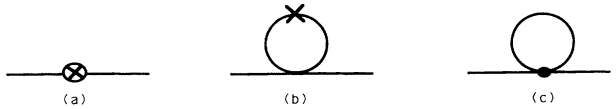

FIG. 7. Renormalization counterterms for second-order calculations: (a) counterterm for Fig. 3(b) and (b) mass and (c) vertex counterterms.

correction to the four-point vertex. However, no harm is done by this additional resummation; all that happens is a redistribution among the diagrams of the next correction at order g^4, as we will soon see.

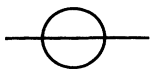

FIG. 8. Overlapping two-loop self-energy diagram.

III. TWO-LOOP DIAGRAMS

The basic diagrams that must be considered to evaluate the self-energy to order g^4 using $\mathcal{L}_3$ are in Figs. 1, 3, 7, and 8. Before delving into the calculations, let us make some observations. Just as for $T=0$, the sum of graphs in Fig. 1 must be UV finite. Also, as for $T=0$, Figs. 7(b) and 7(c) are the mass and vertex counterterm diagrams that are required to cancel the subdivergences arising from the two-loop diagrams Figs. 3(a) and 8. A "new" [6] feature of the resummation is the counterterm of Fig. 7(a) which is needed to cancel UV divergences generated by loop corrections [Fig. 3(b)] to the two-point vertex [Fig. 1(c)].

The sum of diagrams in Fig. 1, evaluated from the Lagrangian $\mathcal{L}_3$, is

$$\begin{aligned}\Pi_4^{(1)}(p^\mu)&=M_3^2-\frac{g^2\mu^{2\epsilon}}{2}\mathrm{Tr}_k\Delta_3(K)-\frac{g^2}{2}\frac{M_3^2}{(4\pi)^2}\frac{1}{\epsilon}\\&=M_3^2-m^2\left[1-\frac{3m}{\pi T}-\frac{3}{4\pi^2}\left[\frac{m}{T}\right]^2\ln\left[\frac{m}{T}\right]^2-\frac{3}{\pi}\left[\frac{m}{T}\right]^2\left[C_1-\frac{3}{2\pi}\right]\right]\\&\quad+\frac{1}{2}\left[\frac{gm}{4\pi}\right]^2\left[\ln\left[\frac{4\pi\mu^2}{m^2}\right]+(1-\gamma_E)\right]+O(g^5\ln g)\,,\end{aligned}\tag{3.1}$$

where γ_E is the Euler constant and $C_1=\frac{1}{4}(2\gamma_E-2\ln 4\pi-1)$. Equations (2.12) and (A4) were used to get the final form (3.1).

Figure 3 contributes

$$\Pi_4^{(3)}(p^\mu)=\frac{g^2\mu^{2\epsilon}}{2}\mathrm{Tr}_q[\Delta_3(Q)]^2\left[\frac{g^2\mu^{2\epsilon}}{2}\mathrm{Tr}_k\Delta_3(K)-M_3^2\right]\,.\tag{3.2}$$

Since

$$(g^2/2)\mathrm{Tr}_k\Delta_3(K)=M_3^2+O(g^4\ln g)\,,$$

therefore the finite part of (3.2) is $O(g^5\ln g)$. In the last section, working with $\mathcal{L}_2$, it was shown that the same diagrams sum to $O(g^4)$. The sum has now been pushed to higher order because of the further resummation performed to obtain $\mathcal{L}_3$. This is an example of the "redistribution" mentioned at the end of the last section—the "lost" contribution from Fig. 3 has been picked up by Fig. 1(a): This is indicated in (3.1) by the presence of the factor $(C_1-3/2\pi)$ rather than C_1, the latter factor being the contribution if $\mathcal{L}_2$ were used in calculating Fig. 1. The diagrams of Fig. 3 are thus only needed to complete the UV renormalization of the theory, which, as usual, is performed loopwise.

The only other graph that is relevant for discussion is given in Fig. 8; it will be considered later. The daisylike diagrams (with $N\geq 2$) were already shown in the last section to be irrelevant at $O(g^4)$. However, now a new infinite set of graphs must be analyzed, the simplest of which are shown in Fig. 9. Each of the diagrams in Fig. 9 is of order g^4 by power counting, but their sum is clearly $O(g^6\ln g)$. Extending diagram 9(a) by adding a bubble (or blob) to its top gives a graph of order g^5. So one only needs to consider adding N number of bubbles + blobs to the middle loop and M bubbles + blobs to the bottom loop of Fig. 9(a) to create the general "cactus" diagram of order g^4 shown in Fig. 10. It is sufficient to show that the sum of all such cactus diagrams is of order g^5 or higher: First, consider Fig. 10 with the bottom loop and its M attachments fixed in a particle configuration. Then any subdiagram (with fixed $N\geq 0$) above the bottom loop is precisely a daisy diagram and these have been shown to sum to $O(g^5)$ at most. For any $M\geq 0$ the bottom loop in Fig. 10 contributes a factor $g^2(1/g)=g$. Hence the sum of all possible cactus diagrams is at most of order g^6.

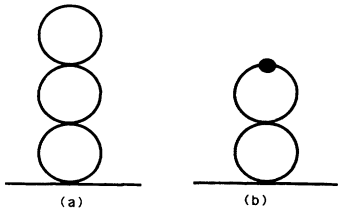

FIG. 9. Diagrams which are individually of order g^4, but sum to order $g^6\ln g$.

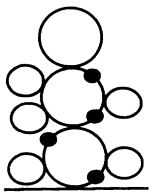

FIG. 10. General "cactus" diagram. $N\geq 0$ bubbles + blobs are attached to the middle loop, while $M\geq 0$ bubbles + blobs are attached to the bottom loop.

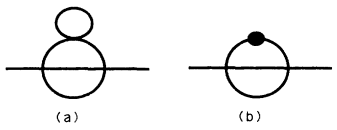

FIG. 11. More complicated self-energy diagrams which are individually of order g^4, but sum to order $g^6\ln g$.

This completes the proof.

Adding bubbles or blobs to Fig. 8 creates diagrams such as those shown in Fig. 11. These sum to order $g^6\ln g$. All other diagrams are individually of order $g^5\ln g$ or higher.

Having accounted for all the relevant diagrams, let us return to some explicit results. The counterterms in Fig. 7 contribute

$$\Pi_4^{(7)}=\left[\frac{gM_3}{4\pi}\right]^2\frac{1}{2\epsilon}+\frac{g^2\mu^{2\epsilon}}{2}\left[\left[\frac{gM_3}{4\pi}\right]^2\frac{1}{2\epsilon}\right]\mathrm{Tr}_k[\Delta_3(K)]^2-\frac{g^2\mu^{2\epsilon}}{2}\left[\frac{3g^2}{(4\pi)^2}\frac{1}{2\epsilon}\right]\mathrm{Tr}_k\Delta_3(K)\ . \tag{3.3}$$

Summing (3.2) and (3.3) gives

$$\Pi_4^{(3,7)}=\frac{-g^4}{2\epsilon}\frac{I_\beta^\epsilon(M_3)}{(4\pi)^2}-\frac{g^4}{2\epsilon}\frac{M_3^2}{(4\pi)^4}\left[(\gamma_E-1)-\ln\left[\frac{4\pi\mu^2}{M_3^2}\right]\right]+\frac{3g^4}{4\epsilon^2}\frac{M_3^2}{(4\pi)^4}+\text{finite terms } O(g^5\ln g)\ , \tag{3.4}$$

where

$$I_\beta^\epsilon(M_3)\equiv\mu^{2\epsilon}\int\frac{d^{D-1}k}{(2\pi)^{D-1}}\frac{n_k}{E_k}\ .$$

The first line in (3.4) is a nonrenormalizable temperature-dependent infinity generated by diagrams 3(a) and 7(c). It will cancel [8] when the two-loop overlapping diagram of Fig. 8 is added. This last diagram is the only relevant diagram which depends on the external momentum $(p^0,\mathbf{p})$,

$$\Pi_4^{(8)}(p^0,\mathbf{p})=\frac{g^4\mu^{4\epsilon}}{3!}\mathrm{Tr}_k\mathrm{Tr}_q[\Delta_3(K)\Delta_3(Q)\Delta_3(P-K-Q)]=G_0(p^0,\mathbf{p})+G_1(p^0,\mathbf{p})+G_2(p^0,\mathbf{p})\ , \tag{3.5}$$

where

$$G_0(p^0,\mathbf{p})=\int d[k,q]S(E_k,E_q,E_r)\ , \tag{3.6}$$

$$G_1(p^0,\mathbf{p})=3\int d[k,q]n_k[S(E_k,E_q,E_r)+S(-E_k,E_q,E_r)]\ , \tag{3.7}$$

$$G_2(p^0,\mathbf{p})=3\int d[k,q]n_kn_q[S(E_k,E_q,E_r)+S(-E_k,E_q,E_r)+S(E_k,-E_q,E_r)-S(E_k,E_q,-E_r)]\ , \tag{3.8}$$

with the definitions

$$S(E_k,E_q,E_r)=\left[\frac{1}{ip^0+E_k+E_q+E_r}+\frac{1}{-ip^0+E_k+E_q+E_r}\right],$$

$$d[k,q]=\frac{g^4\mu^{4\epsilon}}{3!}\frac{d^{D-1}k}{(2\pi)^{D-1}}\frac{d^{D-1}q}{(2\pi)^{D-1}}\frac{1}{8E_kE_qE_r}\ ,$$

$$r=|\mathbf{k}+\mathbf{q}-\mathbf{p}|\ ,$$

$$E_l^2=l^2+M_3^2,\quad l=k,q,r\ ,$$

and n_l the usual BE factor. The real-time retarded self-energy follows by making the analytic continuation $p^0\to-i\omega+\xi$ with $\xi=0^+$ [10]. Then the prescription

$$\frac{1}{A\pm i\xi}=P\left[\frac{1}{A}\right]\mp i\pi\delta(A) \tag{3.9}$$

gives the real and imaginary parts of the diagram [14]. Consider first the real part. Since G_0 does not contain any Bose-Einstein factors, it must be the expression for diagram (8) obtained using $T=0$ Feynman rules and with the energy integrals done. In covariant [i.e., with $P^2=-\omega^2+(\mathbf{p})^2$] notation, one gets [15]

$$\mathrm{Re}G_0(P^2)=\mathrm{Re}\frac{g^4\mu^{4\epsilon}}{3!}\int\frac{d^Dk}{(2\pi)^D}\int\frac{d^Dq}{(2\pi)^D}\frac{1}{K^2+M_3^2}\frac{1}{Q^2+M_3^2}\frac{1}{(K+Q-P)^2+M_3^2}$$
$$=\frac{-g^4}{4}\frac{M_3^2}{(4\pi)^4}\left[\frac{1}{\epsilon^2}+\frac{3-2\gamma_E}{\epsilon}+\frac{2}{\epsilon}\ln\left[\frac{4\pi\mu^2}{M_3^2}\right]\right]-\frac{g^4}{4}\frac{P^2}{(4\pi)^4}\frac{1}{6\epsilon}+\text{finite terms } O(g^4M_3^2)(P^2/M_3^2)^2\ . \tag{3.10}$$

For soft external momenta ($P^2\sim m^2$), the region of interest, the finite terms are of order g^6 and so do not contribute to the self-energy at order g^4.

G_1 represents the mixing of the $T=0$ piece from one loop with the $T\neq0$ piece from the second loop. This is clear from the expression (3.7), which contains only one BE factor, making one of the loop integrals UV finite, while the other loop integral has a UV divergence. Speci-

alizing to the case $\mathbf{p}=0$ in order to do the angular integrations, gives (see the Appendix)

$$\mathrm{Re}G_1(-i\omega,0)=F_0+F_1+F_2(\omega^2)\ , \tag{3.11}$$

where

$$F_0=\frac{g^4}{2}\frac{I_\beta^\epsilon(M_3)}{(4\pi)^2}\frac{1}{\epsilon}\ , \tag{3.12}$$

$$F_1=\frac{g^4}{2}\frac{I_\beta^{\epsilon=0}(M_3)}{(4\pi)^2}\left[\ln\frac{4\pi\mu^2}{M_3^2}+2-\gamma_E\right]$$

$$=\left[\frac{gm}{4\pi}\right]^2\left[\ln\frac{4\pi\mu^2}{m^2}+2-\gamma_E\right]+O(g^4\ln g)\ , \tag{3.13}$$

and

$$F_2(\omega^2)=\frac{g^4}{8(2\pi)^4}\int_0^\infty dk\frac{kn_k}{E_k}\int_0^\infty\frac{dq}{E_q}\left[q\ln\left|\frac{X_+}{X_-}\right|-4k\right]\ , \tag{3.14}$$

with

$$X_\pm=[\omega^2-(E_k+E_q+E_{k\pm q})^2][\omega^2-(E_q-E_k+E_{k\pm q})^2]\ .$$

The temperature-dependent infinity F_0 is actually independent of the external momenta p^μ and cancels precisely against a similar term found earlier in Eq. (3.4).

Finally, G_2 contains a BE factor for each loop and so is UV finite. It has, however, a logarithmic IR divergence as $m,\omega\to 0$. One obtains

$$H(\omega^2)\equiv\mathrm{Re}G_2(-i\omega,0)$$
$$=\frac{g^4}{8(2\pi)^4}\int_0^\infty dk\frac{kn_k}{E_k}\int_0^\infty dq\frac{qn_q}{E_q}\ln\left|\frac{Y_+}{Y_-}\right|\ , \tag{3.15}$$

where

$$Y_\pm=[\omega^2-(E_k+E_q+E_{k\pm q})^2][\omega^2-(E_q-E_k+E_{k\pm q})^2]$$
$$\times[\omega^2-(E_k-E_q+E_{k\pm q})^2]$$
$$\times[\omega^2-(E_k+E_q-E_{k\pm q})^2]\ . \tag{3.16}$$

The sum of all UV-divergent terms from Eqs. (3.4), (3.10), and (3.12) gives

$$\left[\frac{g^2}{16\pi^2}\right]^2M_3^2\left[\frac{1}{2\epsilon^2}-\frac{1}{4\epsilon}\right]-\left[\frac{g^2}{16\pi^2}\right]^2\frac{P^2}{24\epsilon}\ . \tag{3.17}$$

These are canceled by the two-loop wave function and mass renormalization counterterms

$$-\frac{1}{2}(\partial_\mu\phi)^2\left[\left[\frac{g^2}{16\pi^2}\right]^2\frac{1}{24\epsilon}\right]$$
$$+\frac{M_3^2}{2}\left[\left[\frac{g^2}{16\pi^2}\right]^2\left[\frac{1}{2\epsilon^2}-\frac{1}{4\epsilon}\right]\right]\ . \tag{3.18}$$

The temperature-dependent UV mass counterterm in (3.18) is $O(g^6)$. As before, it will precisely compensate [16] the $O(g^6)$ temperature-dependent UV counterterm for the two-point interaction [the diagrams that require the latter counterterm are formed by adding a blob to Figs. 3(a), 7(b), 7(c), and 8].

The real part of the renormalized self-energy for $\mathcal{L}_3$ is therefore [Eqs. (3.1) and (3.13)–(3.15)]

$$R(\omega^2)\equiv\mathrm{Re}\Pi_4^{\mathrm{ren}}(-i\omega,0)$$
$$=\Pi_4^{(1)}+F_1+F_2(\omega^2)+H(\omega^2)$$
$$+\text{terms of order }(g^5\ln g)\ . \tag{3.19}$$

This expression contains all corrections at order g^4. It also contains some effects at order g^5 and higher in the energy-dependent terms F_2 and H. For general ω, the expressions $F_2(\omega)$ and $H(\omega)$ are too complicated to evaluate in closed form. However, since only contributions to $O(g^4)$ are required, something can be said. Note that because of the explicit factor of g^4 it is only necessary to identify the IR behavior of the integrals in Eqs. (3.14) and (3.15) to obtain information about the leading contribution. Clearly, the ω dependence of any IR behavior in F_2 or H can only be possible for ω soft ($\sim m$). Consider first $F_2(\omega^2)$. It is easy to see that the logarithmic IR singularity as $m,\omega\to 0$ is due to the second factor in the term X_- in the region $k\geq q$. So one is led to investigate the piece

$$\int_0^\infty\frac{x\,dx}{E_x}n_x\int_0^x\frac{y\,dy}{E_y}\ln[(E_y+E_{x-y}-E_x)^2-\sigma^2]\ , \tag{3.20}$$

where I have factored out T^2 and defined the set of dimensionless variables $\{x,y,a,\sigma\}$ by scaling the quantities $\{k,q,m,\omega\}$, respectively, by $1/T$. Now, for $a\to 0$, the estimate

$$(E_y+E_{x-y}-E_x)^2\sim\vartheta(a^4)[1/y+1/(x-y)-1/x]^2$$

holds. From this it can be deduced that for $\sigma\sim a^n\sim g^n$ the "leading-log" contribution from (3.20) goes like $2\ln a^2$ for $n>2$ and like $n\ln a^2$ for $n<2$. For $H(\omega^2)$, the logarithmic IR singularity is caused by the extra BE factor, while the magnitude of its contribution is controlled by the $\ln(Y_+/Y_-)$ term. Writing

$$\frac{Y_\pm}{T^8}=-(8xy)^2(x\pm y)^2\sigma^2+(a^2-\sigma^2)^2Z_\pm\ , \tag{3.21}$$

where

$$Z_\pm=16[(x\pm y)^2(x^2+y^2)+(xy)^2+a^2(x^2+y^2\pm xy)]$$
$$+8(a^2-\sigma^2)(x^2+y^2+a^2\pm xy)+(a^2-\sigma^2)^2\ ,$$

shows that the first term in (3.21) dominates for $\sigma\sim a$, while the transition to more complicated behavior is again at $\sigma\sim ga\sim g^2$.

To get the full g^4 dependence from F_2 and H, the constant under the leading $g^4\ln g$ contribution is also needed. This can be done for specific values of ω when it is possible to isolate clearly the $O(g^4)$ pieces from the partial higher-order effects. A calculation, which is sketched in the Appendix, gives [with corrections at $O(g^5)$ omitted]

$$F_2(0)=\lambda\frac{\pi}{\sqrt{3}}\ ,$$
$$H(0)=\lambda\left[\ln\left[\frac{m}{T}\right]^2+3.488\,71...\right]\ ,$$
$$F_2(M_3^2)=\lambda\left[-\frac{1}{2}\ln\left[\frac{m}{T}\right]^2+0.545\,97...\right]\ , \tag{3.22}$$
$$H(M_3^2)=\lambda\left[\frac{3}{2}\ln\left[\frac{m}{T}\right]^2+4.520\,97...\right]\ ,$$

from which follows

$$F_2(0)+H(0)=\lambda\left[\ln\left[\frac{m}{T}\right]^2+5.3025...\right]\ ,$$
$$F_2(M_3^2)+H(M_3^2)=\lambda\left[\ln\left[\frac{m}{T}\right]^2+5.0669...\right]\ , \tag{3.23}$$

where $\lambda=-(gm/4\pi)^2$. Surprisingly, from (3.23) it appears that the coefficient in front of the total $O(g^4\ln g)$ contribution to the real self-energy (3.19) from the energy-dependent part is the same on shell as for zero external four-momentum. Let me now proceed to the determination of the pole of the effective propagator. The complex pole Ω at zero momentum ($\mathbf{p}=0$) is the zero of the equation

$$-\Omega^2+M_3^2-\Pi_4^{\rm ren}(-i\omega,0)=0\ . \tag{3.24}$$

Since $\mathrm{Im}\Pi_4(-i\Omega,0)$ is $O(g^4)$ (see later), then by writing $\Omega=\omega-i\gamma$, the real part of the pole up to $O(g^4)$ is determined by

$$-\omega^2+M_3^2-R(\omega^2)=0\ . \tag{3.25}$$

The above equation may be solved by iteration (see the Appendix) to give the thermal mass M_4 up to order g^4:

$$M_4^2=M_3^2-R(M_3^2)\ , \tag{3.26}$$

where the right-hand side must be expanded up to order g^4. Using the values for $F_2(M_3^2)$ and $H(M_3^2)$ given in (3.23), together with Eqs. (3.1), (3.13), and (3.19), in (3.26) above give the final answer

$$M_4^2=m^2\left[1-\frac{3m}{\pi T}\right]+\left[\frac{gm}{4\pi}\right]^2\left[\frac{3}{2}\ln\frac{T^2}{4\pi\mu^2}+2\ln\left[\frac{m}{T}\right]^2\right]+\alpha\left[\frac{gm}{4\pi}\right]^2\ , \tag{3.27}$$

where $\alpha=14.1416...$ and m^2 is defined by Eq. (2.7). Taking the square root of the above expression gives the complete thermal mass up to order g^3.

The imaginary part [14] of the self-energy to order g^4 is due only to the two-loop diagram of Fig. 8. From (3.5)–(3.9), it is relatively simple to obtain the imaginary part at zero momentum and on shell:

$$\mathrm{Im}\Pi_4^{(8)}(-iM_3,0)=\frac{g^4}{16}\left[\frac{1}{2\pi}\right]^3\int_0^\infty dk\frac{k\eta_k}{E_k}\int_0^k\frac{q\,dq}{E_q}$$
$$=\frac{g^2m^2}{32\pi}+O(g^5)\ . \tag{3.28}$$

The result, as expected on general grounds [12], is positive. The imaginary part could also have been obtained directly, without using the prescription (3.9), by keeping the full logarithm in (3.14) and (3.15) instead of only its principal value. Finally, the damping rate follows from (3.24):

$$\gamma=\frac{\mathrm{Im}\Pi_4^{(8)}(-iM_3,0)}{2M_3}$$
$$=\frac{g^2m}{64\pi}+O(g^4)\ . \tag{3.29}$$

IV. CONCLUSION

To summarize, the effective expansion created by a resummation in the original theory was used to obtain the zero-momentum pole of the propagator consistently to order g^4. Working order by order in the effective expansion, the relevant diagrams were identified and perturbative computability was shown to hold by explicitly verifying the cancellation of contributions from an infinite class of diagrams.

The first resummation of self-energy diagrams to get the effective Lagrangian $\mathcal{L}_2$ was essential because the thermal mass at lowest order, m, is as large as the inverse massless propagator at soft momenta. That is, the thermal mass could not be treated as a perturbation. As pointed out in the text, the second resummation to form $\mathcal{L}_3$ was not really necessary since the order-g^3 correction to m^2 is a perturbative effect. The consequence of the second resummation was simply to change the individual contributions for some of the diagrams at $O(g^4)$. In particular, whereas the diagrams in Fig. 3 would have been relevant if we had continued using $\mathcal{L}_2$, they became irrelevant when $\mathcal{L}_3$ was used—this "lost" contribution was compensated by new subleading contributions from the diagrams in Fig. 1. In short, though the reader could have been spared any mention of $\mathcal{L}_3$, nevertheless the author feels that some insight into the effects of resummation was gained by the exercise.

Let me now make some comparisons with results in the literature. In [6] a mass parameter was introduced in the beginning and the effective mass was defined by requiring that the corrections to the free inverse propagator vanish at zero external four-momenta. Translating that into the language of this paper simply amounts to using $R(0)$ on the right-hand side of (3.26) rather than $R(M_3^2)$. In general, by definition, this does not give the pole in the propagator. From (3.23) we see that the difference between the two definitions shows up in the constant under the logarithm at order $g^4\ln g$ (in the Appendix, I explain the difference). I do not know, however, whether it is a coincidence that the coefficients of the "logs" in (3.23) are the same. The imaginary part of the self-energy, of course,

vanishes for $\omega=0$, as is apparent from (3.5)–(3.9) or from more general arguments [12], but is given on shell by (3.28).

Clearly, any quantity calculated in either the RTF or ITF must give the same result, even though some of the intermediate expressions may look different because of the differences in approach. For completeness, I have checked (using the real-time expressions found in [5] and [6]) up to order g^4 that the two formalisms give identical answers for the pole of the propagator and also when used to calculate the effective mass as defined in [6].

For gauge theories both the one-loop self-energy and vertices must be resummed into effective quantities [3]. Since these quantities are momentum dependent, the effective expansion is quite involved even at one-loop order. Nevertheless, one expects that some of the features of two-loop calculations studied here in a simpler context will also manifest themselves in gauge theories.

ACKNOWLEDGMENTS

I gratefully acknowledge Dr. R. D. Pisarski for suggesting the problem and for the many subsequent discussions and helpful comments and Professor M. Roček for his valuable advice and support. I also thank Professor J. C. Taylor for pertinent questions and comments concerning temperature-dependent counterterms. Finally, the author thanks C. Corianò, G. Estefan, and R. Stewart for inspiring and encouraging conversations. This work was supported in part by NSF Grant No. PHY 91-08054.

APPENDIX

(1) The basic expression appearing in one-loop diagrams is

$$\mu^{2\epsilon}\mathrm{Tr}\Delta_k(K)\equiv I_0(M)+I_\beta^\epsilon(M)\ , \tag{A1}$$

with

$$I_0(M)=\mu^{2\epsilon}\int\frac{d^{D-1}k}{(2\pi)^{D-1}}\frac{1}{2E_k} =\frac{M^2}{(4\pi)^2}\left[\frac{4\pi\mu^2}{M^2}\right]^\epsilon\Gamma(-1+\epsilon)\ , \tag{A2}$$

$$I_\beta^\epsilon(M)=\mu^{2\epsilon}\int\frac{d^{D-1}k}{(2\pi)^{D-1}}\frac{n_k}{E_k}\ . \tag{A3}$$

For $(M/T)\ll 1$, we have the expansion [13]

$$I_\beta^{\epsilon=0}(M)=\frac{T^2}{12}\left[1-\frac{3M}{\pi T}-\frac{3}{4\pi^2}\left[\frac{M}{T}\right]^2\ln\left[\frac{M}{T}\right]^2 -\frac{3}{\pi}\left[\frac{M}{T}\right]^2\left[\frac{\gamma_E}{2}-\frac{\ln 4\pi}{2}-\frac{1}{4}\right]\cdots\right]\ . \tag{A4}$$

The expression $\mu^{2\epsilon}\mathrm{Tr}[\Delta(K)]^2$ can be obtained by differentiating (A1)–(A3) with respect to M^2.

(2) To get (3.11)–(3.14). Consider the q integrals in (3.7). For $\mathbf{p}=0$ the only nontrivial angular integral in $D-1$ dimensions is for the angle θ between $\mathbf{k}$ and $\mathbf{q}$. Choose $\mathbf{k}$ to define the polar axis, and first do the trivial angular integrals for the q variables (see [9], for example, for the correct measure for the integrals in D dimensions). Then one is left with the integral ($t=\cos\theta$)

$$\int_0^\infty\frac{dq}{E_q}q^{1-2\epsilon}L(k,q)\ , \tag{A5}$$

where

$$L(k,q)=\int_{-1}^{1}dt\frac{1}{(1-t^2)^\epsilon}\frac{\partial}{\partial t} \times\{\ln[\omega^2-(E_q+E_r-E_k)^2] \times[\omega^2-(E_q+E_r+E_k)^2]\}\ . \tag{A6}$$

The simplest way to proceed is to subtract the UV-divergent part of (A5). As $q\to\infty$, $(\partial/\partial t)(\ )\to 2k/q$. Subtracting and adding this term at the appropriate place in (A6), substituting everything back in (A5) and (3.7), and then doing the obvious simplification gives the result quoted in the text.

(3) Solving Eq. (3.25). Since $M_3^2\sim O(g^2)$ and $R(\omega^2)\sim O(g^4)$, a consistent way to solve (3.25) is by iterating the lowest-order solution $\omega_0^2=M_3^2$. The next iteration gives the result in the text [Eq. (3.26)], while further iteration will give a correction at $O(g^6)$. Essentially, then, the pole is determined by the self-energy on mass shell. Now consider a Taylor expansion of $R(\omega^2)$ about $\omega^2=0$. Since R has a logarithmic IR singularity as $\omega,m\to 0$ (see text), therefore

$$R(\omega^2)=\sum_{n=0}^{\infty}\frac{(\omega^2)^n}{n!}\left.\frac{\partial^n R(\omega^2)}{\partial(\omega^2)^n}\right|_{\omega^2=0} \sim g^4\vartheta\left[\sum_n\frac{\omega^{2n}}{(m^{2n})n!}\right]\ . \tag{A7}$$

For ω soft ($\sim m$), the Taylor expansion is *not* an expansion in g as each term is of order g^4. So one should expect $R(0)$ and $R(\omega^2)$ to differ by an amount $O(g^4)$ [see (3.23)]. The same argument explains why it would be difficult to obtain the full order-g^4 contribution to the self-energy at soft nonzero external momentum ($\mathbf{p}$) by doing a Taylor expansion about $\mathbf{p}=0$.

(4) To obtain (3.22). To extract the leading "lng +const" contribution from the integrals appearing in (3.14) and (3.15), the following procedure is adopted: Identify the terms which will contribute the ln$m$ singularities, isolate them, and then set $m=0$ in the regular terms to get pieces of the $O(g^4)$ contribution. Next, simplify the potentially singular terms and keep repeating the above procedure until all the "log+const" pieces have been explicitly obtained. Consider, for example, $F_2(\omega^2=M_3^2)$. The term within parentheses in (3.14) is simplified (for ω on shell) and written (replacing M_3 with m in the expressions F_2 and H ignores a correction of order g^5) as

$$q \ln \left[\left[\frac{q+k}{q-k} \right] \left[\frac{m^2+q(q+k)+E_q E_{q+k}}{T^2} \right] \right] \tag{A8}$$

$$-q \ln \left| \frac{m^2+q(q-k)+E_q E_{k-q}}{T^2} \right| \tag{A9}$$

$$-4k \ . \tag{A10}$$

As discussed in the text, there are no IR singularities in the region $q \geq k$, and so one may set $m=0$ in the above expressions in that range of integration. For the $q \leq k$ sector, (A9) and (A10) both contribute "logs," while (A8) gives a finite piece in the massless limit. For the piece in (A10), the q integration is easily done explicitly; then the $\ln m$ piece is isolated and the finite terms determined. For (A9) multiply the argument of the logarithm by $[m^2+q(q-k)-E_q E_{k-q}]$ in the numerator and denominator, simplify, isolate the "log" piece, and set $m=0$ in the rest to get the constants. Collecting all the terms gives

$$F_2(M_3^2)=\frac{g^4}{6}\frac{T^2}{64\pi^2}\left[\frac{1}{2}\ln\left[\frac{m}{T}\right]^2-\ln 2-\frac{6}{\pi^2}\int_0^\infty dx\frac{x\ln x}{e^x-1}\right]+O(g^5\ln g) \ . \tag{A11}$$

The integral in the final answer (A11) is a pure number. It may be computed numerically if required. The concise result is given in the text [Eq. (3.22)].

For a different example, consider

$$H(M_3^2)=2\frac{g^4}{64\pi^4}\int_0^\infty dk\frac{kn_k}{E_k}\int_0^k dq\frac{qn_q}{E_q}\ln\left|\frac{k+q}{k-q}\right| \ , \tag{A12}$$

where the symmetry of the integrand under $k \leftrightarrow q$ interchange has been exploited to restrict the range of one of the integrals. As the IR singularity is now due to the extra BE factor rather than the explicit logarithm, the "log+const" pieces can be obtained by using an arbitrary soft cutoff Λ (I thank R. D. Pisarski for suggesting this technique) to divide the region of integration for the k variable. For $k \leq \Lambda$ the appropriate approximation can be made (e.g., $n_k = 1/E_k$) to simplify the integrations. In the limit $a \to 0$, one gets, for $k \leq \Lambda$ in (A12),

$$T^2\left[\frac{-\pi^2}{4}\ln\left[\frac{m}{T}\right]+\frac{\pi^2}{4}\ln\left[\frac{\Lambda}{T}\right]+\int_0^1 dt\ln\left|\frac{1+t}{1-t}\right|\frac{\ln t}{(t-t^3)}\right]+O(m)+O(\Lambda) \ . \tag{A13}$$

For the region $k \geq \Lambda$, one can put the mass to zero because there are no $\ln m$ singularities. Next, isolate the $\ln\Lambda$ factor (for $\Lambda \to 0$) by doing a subtraction of the leading IR part of one of the BE factors, to get, finally for $k \geq \Lambda$ in (A12),

$$T^2\left[-\frac{\pi^2}{4}\ln\left[\frac{\Lambda}{T}\right]+\int_0^1 dt\int_0^\infty dx\frac{x}{e^x-1}\left[\frac{1}{e^{xt}-1}-\frac{1}{xt}\right]\ln\left|\frac{1+t}{1-t}\right|\right]+O(m)+O(\Lambda) \ . \tag{A14}$$

In the limit $\Lambda \to 0$, the sum of (A13) and (A14) gives the final answer for (A12), with neglected terms of order g^5. The cancellation of the $\ln\Lambda$ terms in the sum removes the ambiguity coming from the cutoff.

Similar considerations as above give

$$F_2(0)=-\frac{g^4}{6}\frac{T^2}{64\pi^2}\frac{\pi}{\sqrt{3}}+O(g^5) \ , \tag{A15}$$

$$\begin{aligned} H(0)=&-\frac{g^4}{6}\frac{T^2}{64\pi^2}\ln\left[\frac{m}{T}\right]^2+\frac{g^4T^2}{32\pi^4}\int_0^1 dt\frac{\ln t}{t-t^3}\ln\left[\frac{1+t+t^2}{1-t+t^2}\right] \\ &+\frac{g^4T^2}{32\pi^4}\int_0^1 dt\int_0^\infty dx\frac{x}{e^x-1}\left[\frac{1}{e^{xt}-1}-\frac{1}{xt}\right]\ln\left[\frac{1+t+t^2}{1-t+t^2}\right] \\ &+\frac{g^4T^2}{32\pi^4}\int_0^1 dt\int_0^\infty dx\frac{tx^3}{(x^2+1)(x^2t^2+1)}\ln\left[\frac{4x^2+\frac{3}{1+t+t^2}}{4x^2+\frac{3}{1-t+t^2}}\right]+O(g^5) \ . \end{aligned} \tag{A16}$$

Again, if necessary, the constant integrals appearing above can be done numerically to give the result in (3.22).

[1] A. Linde, Rep. Prog. Phys. **42**, 389 (1979); D. J. Gross, R. D. Pisarski, and L. G. Yaffe, Rev. Mod. Phys. **53**, 43 (1981).

[2] S. Weinberg, Phys. Rev. D **9**, 3357 (1974).

[3] R. D. Pisarski, Phys. Rev. Lett. **63**, 1129 (1989); E. Braaten and R. D. Pisarski, Nucl. Phys. **B337**, 569 (1990); R. D. Pisarski, in *Quark Matter 90,* Proceedings of the Conference, Menton, France, 1990, edited by J. P. Blaizot

et al. [Nucl. Phys. **A525** (1991)].
[4] See, for example, E. Braaten and T. C. Yuan, Phys. Rev. Lett. **66**, 2183 (1991), and references therein.
[5] T. Altherr, Phys. Lett. B **238**, 360 (1990).
[6] N. Banerjee and S. Mallik, Phys. Rev. D **43**, 3368 (1991).
[7] S. P. Chia, Int. J. Mod. Phys. A **2**, 713 (1987); P. Fendley, Phys. Lett. B **196**, 175 (1987).
[8] M. B. Kislinger and P. D. Morley, Phys. Rev. D **13**, 2771 (1976); H. Matsumoto, I. Ojima, and H. Umezawa, Ann. Phys. (N.Y.) **152**, 348 (1984).
[9] B. de Wit and J. Smith, *Field Theory in Particle Physics* (North-Holland, Amsterdam, 1986).
[10] A. A. Abrikosov, L. P. Gorkov, and I. E. Dzyaloshonski, *Methods of Quantum Field Theory in Statistical Physics* (Dover, New York, 1975).
[11] J. Kapusta, *Finite Temperature Field Theory* (Cambridge University Press, Cambridge, England, 1985).
[12] R. D. Pisarski, Nucl. Phys. **B309**, 476 (1988).
[13] L. Dolan and R. Jackiw, Phys. Rev. D **9**, 3320 (1974).
[14] H. A. Weldon, Phys. Rev. D **28**, 2007 (1983).
[15] E. Mendels, Nuovo Cimento **45**, 87 (1978).
[16] It is well known that no temperature-dependent counterterms are required in bare perturbation theory [8]. The same is true for the net Lagrangian (even with a possible nonzero $T=0$ mass) in the resummed expansion if a mass-independent renormalization scheme is used. The latter fact is transparent in the approach used in [6].